Eur. Phys. J. C 12, 451–460 (2000)
Digital Object Identifier (DOI) 10.1007/s100529900266

THE EUROPEAN PHYSICAL JOURNAL C

Yukawa coupling corrections to the decay $H^+ \to W^+ A^0$

A. Akeroyd[1,a], A. Arhrib[2,3,4,b], E. Naimi[3,4]

[1] Departamento de Física Teórica, IFIC/CSIC, Universidad de Valencia, 46100 Burjassot, Valencia, Spain
[2] Departemento de Fisica-CENTRA, Instituto Superior Técnico, Av Rovisco Pais 1, 1096 Lisboa Codex, Portugal
[3] Département de Mathématiques, Faculté des Sciences et Techniques, B.P 416, Tanger, Morocco
[4] UFR-High Energy Physics, Physics Departement, Faculty of Sciences, PO Box 1014, Rabat, Morocco

Received: 22 April 1999 / Published online: 10 December 1999

Abstract. We compute the fermionic radiative contributions to the decay $H^+ \to W^{+(*)} A^0$ in the framework of models with two Higgs doublets (2HDM), for the case of an on-shell and off-shell W. We show that, in the majority of the cases, current measurements of the ρ parameter suggest $M_{H^\pm} \geq M_A$ and such decays could invalidate current charged Higgs searches or aid detection in the region $M_{H^\pm} \approx M_W$. We find that the radiative corrections may approach 50% for small values of $\tan\beta$.

1 Introduction

The search for the Higgs boson (ϕ^0)[1] of the standard model (SM) [2] is one of the major challenges for present and future colliders. In recent years there has been growing interest in the study of extended Higgs sectors with more than one Higgs doublet [3]. The simplest extension is the two Higgs doublet model (2HDM), and such a structure is required for the minimal supersymmetric standard model (MSSM). Models with two (or more) Higgs doublets predict the existence of charged Higgs bosons, and their discovery would be conclusive evidence of an extended Higgs sector. In the 2HDM extension of the SM, from the eight degrees of freedom initially present in the two Higgs doublets, only five remain after the electroweak symmetry breaking and should become manifest as physical particles: two charged Higgs scalars ($H^\pm$), two CP even scalars (h^0 and H^0) and one CP odd scalar (A^0). Accurate predictions for the branching ratios (BR) of these particles are required in order to facilitate the searches and in this paper we consider the radiative corrections to the decay $H^\pm \to A^0 W^{(*)}$. In the non-supersymmetric 2HDM (hereafter to be called simply 2HDM), the masses M_A and $M_{H^\pm}$ may be taken as free parameters, so one may consider both the case of an off-shell and on-shell W. This is in contrast to the MSSM in which M_A and $M_{H^\pm}$ are correlated and the two-body decay is never allowed. We shall show that current measurements of the ρ parameter strongly suggest $M_{H^\pm} \geq M_A$ for $M_{H^\pm} \geq 100\,\mathrm{GeV}$.

Recently it has been shown that the decay $H^\pm \to A^0 W^*$ may be dominant or even close to 100% in the 2HDM (Model I) over a wide range of parameter space relevant at LEP-II [4]. This would affect current charged Higgs searches at LEP-II [5,6] and the Tevatron [7] which only assume the decays $H^\pm \to \tau\nu_\tau$ and cs. We therefore feel that it is important to calculate the fermionic radiative corrections to this potentially strong tree-level process. An additional opportunity to use the three-body decay would be the possibility of detection in the difficult $M_{H^\pm} \approx M_W$ region, which is considered marginal if $H^\pm$ conventionally decays to two fermions. Although a thorough analysis is beyond the scope of this paper, the three-body decay would give rise to high multiplicity signatures of more than four jets, with a possibility of detection above the strong WW background. We note that the 2HDM with the popular Model II type structure cannot possess a $H^\pm$ in the discovery range of LEP-II due to constraints from $b \to s\gamma$ [8] (see also [9] which derives the lower bound $M_{H^\pm} \geq 165\,\mathrm{GeV}$), while $H^\pm$ in Model I avoids such constraints and so may be light. We note that it is possible to have the Model II type structure and weaken the above bound on $M_{H^\pm}$ in a 2HDM which relaxes natural flavor conservation (NFC) [10] or a general model with $N(\geq 3)$ doublets [11]. In this paper we are concerned with the 2HDM which imposes NFC. Limits on $M_{H^\pm}$ from the Tevatron are $\tan\beta$ dependent since one requires a significant BR($t \to H^+ b$) in order to obtain a visible signal. In the 2HDM with the Model II type structure this BR can be significant for small (≤ 1) or large (≥ 40) values of $\tan\beta$. For the Model I type structure this is only possible at low $\tan\beta$.

Current mass bounds from LEP-II for the A^0 of the MSSM force $M_{H^\pm} \geq 110\,\mathrm{GeV}$ in this model, thus taking $H^\pm$ out of the LEP-II discovery range [12]. In addition, a recent analysis of the MSSM charged Higgs contributions to $b \to s\gamma$ [13] requires $M_{H^\pm} \geq 110\,\mathrm{GeV}$, a limit valid in both the MSSM and its simplest extension by adding a Higgs singlet superfield (NMSSM). Therefore, from the

[a] e-mail: akeroyd@ccthmail.kek.jp
[b] e-mail: arhrib@fstt.ac.ma

point of view of charged Higgs phenomenology at LEP-II one may consider the 2HDM (Model I) but not more popular extended structures. We will present results for the case of W on shell and off shell for charged Higgs masses of interest at LEP-II and the LHC.

This paper is organized as follows. In Sect. 2 we introduce our notation and the models in question. In Sect. 3 we evaluate the fermionic one loop corrections for the case of an on-shell and off-shell W, while Sect. 4 displays the counterterms. In Sect. 5 we present our results, and Sect. 6 contains our conclusions.

2 Notation, couplings and lowest order results

2.1 Notation and relevant couplings

In this paper we will use the following notation and conventions. The momentum of the charged Higgs boson H^+ is denoted by p_H (p_H is incoming), p_W is the momentum of the W^+ gauge boson and p_A the momentum of the CP odd A^0 (p_W and p_A are outgoing).

The relevant part of the lagrangian describing the interaction of the $W^\pm$ with $H^\pm$ and A^0, comes from the covariant derivative and is given by

$$\mathcal{L} = \frac{e}{2s_W} W_\mu^+ (H^- \overset{\leftrightarrow}{\partial}{}^\mu A^0) + \text{h.c.} \tag{2.1}$$

This interaction is model independent (SUSY or non-SUSY) and it depends only on standard parameters: the electric charge (e) and the Weinberg angle ($s_\text{W} = \sin\theta_\text{W}$).

As we are concerned with the fermionic one loop corrections, we will below give the relevant couplings. In the 2HDM there exist four different ways to couple the Higgs fields to matter (we assume natural flavor conservation [14]). The two most popular are: Model I: The quarks and leptons couple only to one of the two Higgs doublet exactly as in the minimal standard model. Model II: To avoid the problem of flavor changing neutral currents (FCNC), one assumes that one of the two Higgs fields couples only to down quarks (and charged leptons) and the other one couples to up quarks (and neutral leptons). Model type II is the pattern found in the MSSM.

In general, the couplings of the charged Higgs boson $H^\pm$, the Goldstone $G^\pm$, the CP odd A^0 and the gauge boson $W^\pm$ to a pair of fermions are

$$\begin{aligned}
H^+ u\bar{d} &= Y_{ud}^\text{L} \frac{(1-\gamma_5)}{2} + Y_{ud}^\text{R} \frac{(1+\gamma_5)}{2}, \\
G^+ u\bar{d} &= G_{ud}^\text{L} \frac{(1-\gamma_5)}{2} + G_{ud}^\text{R} \frac{(1+\gamma_5)}{2}, \\
A^0 u\bar{u} &= Y_{uu}\gamma_5, \quad A^0 d\bar{d} = Y_{dd}\gamma_5, \\
W_\mu^+ u\bar{d} &= -\text{i}\frac{gV_{ud}}{\sqrt{2}}\gamma_\mu \frac{(1-\gamma_5)}{2}.
\end{aligned} \tag{2.2}$$

Here $u(d)$ may refer to any generation of up (down) quark and the Y couplings are defined as follows:

$$\begin{aligned}
Y_{ud}^\text{L} &= \frac{\text{i}gV_{ud}m_u}{\sqrt{2}M_W \tan\beta}, \quad Y_{ud}^\text{R} = -\frac{\text{i}gV_{ud}m_d}{\sqrt{2}M_W \tan\beta} \quad \text{Model I}, \\
Y_{ud}^\text{L} &= \frac{\text{i}gV_{ud}m_u}{\sqrt{2}M_W \tan\beta}, \quad Y_{ud}^\text{R} = \frac{\text{i}gV_{ud}m_d \tan\beta}{\sqrt{2}M_W}, \quad \text{Model II}, \\
Y_{uu} &= -\frac{gm_u}{2M_W \tan\beta}, \quad Y_{dd} = \frac{gm_d}{2M_W \tan\beta}, \quad \text{Model I}, \\
Y_{uu} &= -\frac{gm_u}{2M_W \tan\beta}, \quad Y_{dd} = -\frac{m_d g \tan\beta}{2M_W}, \quad \text{Model II}, \\
G_{ud}^\text{L} &= \frac{gm_u V_{ud}}{\sqrt{2}M_W}, \quad G_{ud}^\text{R} = -\frac{gm_d V_{ud}}{\sqrt{2}M_W}.
\end{aligned} \tag{2.3}$$

V_{ud} is the Kobayashi–Maskawa matrix element which we will take to be diagonal. It is worth noting that Models I and II are not very different for the top–bottom loop corrections at low $\tan\beta$ because the term $m_t/\tan\beta$ will dominate and it is common to both types.

2.2 Lowest order results

The lowest order Feynman diagram for the two-body decay $H^+ \to A^0 W^+$ and for the three-body decay $H^+ \to A^0 W^* \to A^0 f f'$ (where f and f' are different flavors of fermion) are depicted in the following figure:

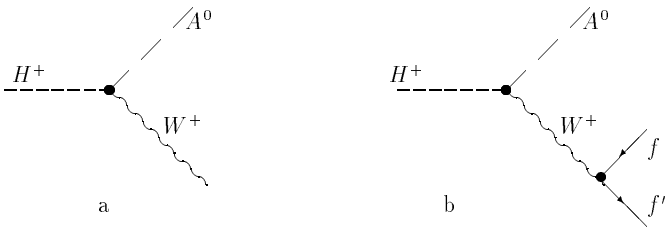

Fig. 1. Feynman diagrams for the Born approximation to the decay $H^+ \to A^0 W^{+*}$, W on shell **a**, W off shell **b**

In the Born approximation, the decay amplitude of the charged Higgs into the *on-shell* CP odd Higgs boson A^0 and the gauge boson W^+ (Fig. 1a) can be written as:

$$\begin{aligned}
\mathcal{M}^0(H^+ \to W^+ A^0) &= \epsilon_\mu^* \Gamma_0^\mu, \quad \text{where} \\
\Gamma_0^\mu &= \text{i}\frac{e}{2s_\text{W}}(p_H + p_A)_\mu.
\end{aligned} \tag{2.4}$$

Here ϵ is the W polarization vector. We then have the following decay width:

$$\Gamma_{on}^0 = \frac{\alpha}{16 s_\text{W}^2 M_W^2 M_{H^\pm}^3} \lambda^{\frac{3}{2}}(M_{H^\pm}^2, M_A^2, M_W^2), \tag{2.5}$$

where $\lambda(x,y,z) = x^2 + y^2 + z^2 - 2(xy + xz + yz)$ is the familiar two-body phase space function. Note that in the MSSM the two-body decay of the charged Higgs boson into $W^+ A^0$ is kinematically not allowed.

Below threshold, and taking into account that the virtual W^* decays into a pair of fermions $f f'$ ($f \neq t$) (Fig. 1b) which we will take to be massless, the Dalitz plot density for this three-body decay $H^+ \to A^0 W^{+*} \to A^0 f f'$ is given by [15]

$$\frac{\text{d}\Gamma_\text{off}^0}{\text{d}x_1 \text{d}x_2} = 9\frac{\alpha^2}{32\pi s_\text{W}^4} M_{H^\pm}$$

$$\times \frac{[(1-x_1)(1-x_2)-\kappa_A]}{([1-x_1-x_2-\kappa_A+\kappa_W]^2+\kappa_W\gamma_W)},$$

where

$$\kappa_{A,W} = \frac{M^2_{A,W}}{M^2_{H^\pm}}, \quad \gamma_W = \frac{\Gamma^2_W}{M^2_{H^\pm}},$$

Γ_W is the total width of the W gauge boson and $x_i = 2E_i/M_{H^\pm}$ are the scaled energies of the massless fermions in the final state. We note that in the non-SUSY 2HDM null searches at LEP in the $e^+e^- \to h^0A^0, h^0Z$ channels eliminate regions in the M_A, M_h plane [6,16]. The excluded region does not have a simple shape, and there are still areas which allow $M_A + M_h \leq 90\,\mathrm{GeV}$. Thus, M_A may be taken as light as 10 GeV. This is in contrast to the MSSM in which one can derive individual lower limits on the masses, of $M_h \geq 70.7\,\mathrm{GeV}$ and $M_A \geq 71.0\,\mathrm{GeV}$ [16]. Therefore, the off-shell decay in the 2HDM can be relevant even for a small $M_{H^\pm}$ ($\leq 80\,\mathrm{GeV}$) in the range at LEP-II.

3 Fermionic radiative corrections

We have evaluated the fermionic radiative corrections to $H^+ \to W^+A^0$ (for both the on-shell and off-shell W) at the one loop level. This set of corrections is ultra-violet (UV) divergent. The UV singularities are treated by dimensional regularization [17] in the on-mass-shell renormalization scheme.

The typical Feynman diagrams for the virtual corrections of order α are drawn in Fig. 2. These comprise the vertex correction (Fig. 2a$_1$, Fig. 2a$_2$), the W^+–W^- self-energy (Fig. 2a$_3$) and the mixed W^+–G^- self-energy (Fig. 2a$_4$). Note that diagrams 2a$_3$ and 2a$_4$ are not to be considered if the gauge boson W is on shell. Figures 2b$_1$,b$_2$,b$_3$ show the fermion loop corrections to $H^\pm$, $G^\pm$ and A^0, respectively. These contributions have to be supplemented by the counterterm renormalizing the vertex $H^+A^0W^-$ (Fig. 2c$_1$), the counterterm for the off-shell W gauge boson self-energy (Fig. 2c$_2$) and by the counterterm for the mixing W–G (Fig. 2c$_3$). These Feynman diagrams are generated and computed using the FeynArts and FeynCalc [18,19] packages. We also use the fortran FF package [20] in the numerical analysis. Note that in the general 2HDM, the vertices $W^+A^0G^-$, $W^+G^0H^-$ and $A^0H^+H^-$ are not present, and so the mixing G^+–H^-, G^0–A^0 and W^+–H^- does not give any contribution to our process.

The one loop amplitude $\mathcal{M}^1$ can be written as

$$\mathcal{M}^1(H^+ \to W^+A^0) = \epsilon^*_\mu \Gamma^\mu. \tag{3.1}$$

Using Lorentz invariance, Γ^μ can be projected as

$$\Gamma^\mu = \frac{e}{2s_\mathrm{W}}(\Gamma_H p^\mu_H + \Gamma_W p^\mu_W). \tag{3.2}$$

Γ_H and Γ_W can be cast as follows:

$$\Gamma_W = \Gamma^{\mathrm{vertex}}_W + \Gamma^{W^+W^-}_W + \Gamma^{W^+G^-}_W + \delta\Gamma^{\mathrm{vertex}}_W + \delta\Gamma^{W^+W^-}_W + \delta\Gamma^{W^+G^-}_W, \tag{3.3}$$

$$\Gamma_H = \Gamma^{\mathrm{vertex}}_H + \Gamma^{W^+W^-}_H + \delta\Gamma^{\mathrm{vertex}}_H + \delta\Gamma^{W^+W^-}_H, \tag{3.4}$$

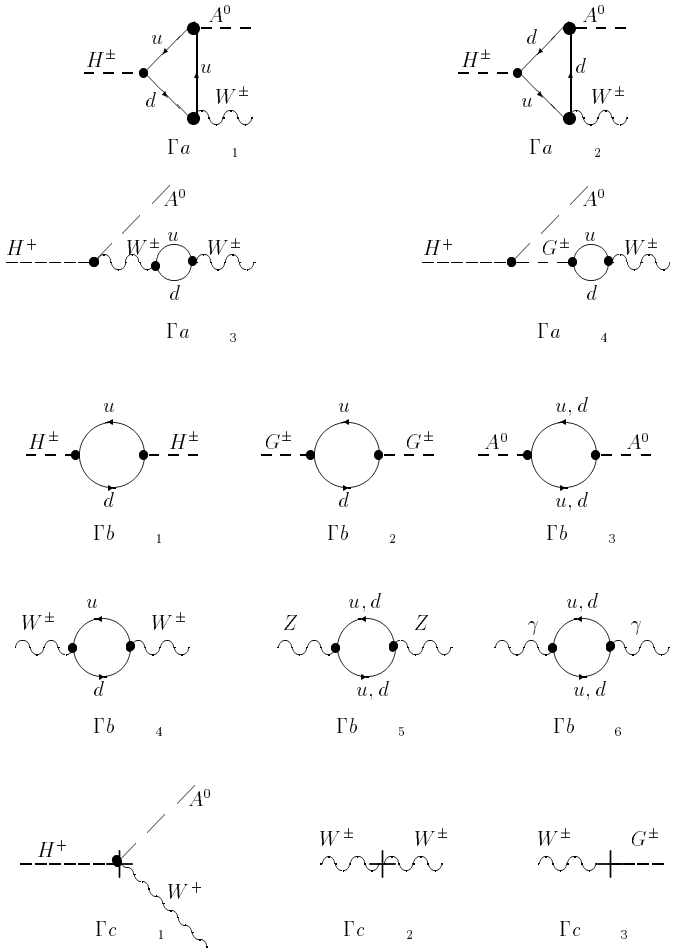

Fig. 2. Feynman diagrams for the one loop corrections to the decay $H^+ \to A^0W^{+*}$: vertex (a$_1$ and a$_2$), WW self-energy (a$_3$), W–G mixing (a$_4$). Charged Higgs boson, Goldstone boson and CP odd self-energies (b$_{1,2,3}$). (b$_{4,5,6}$) WW, ZZ and $\gamma\gamma$ self-energies. (c$_1$) is the vertex counterterm, (c$_2$) W the self-energy counterterm and (c$_5$) is the W–G mixing counterterm

where $\Gamma^{\mathrm{vertex}}_{W,H}$, $\Gamma^{W^+W^-}_{W,H}$ and $\Gamma^{W^+G^-}_W$ are respectively the contribution of the two vertices, the contribution of the self-energy of the W and the contribution of the mixed W^+G^- self-energy; $\delta\Gamma^{\mathrm{vertex}}_{W,H}$, $\delta\Gamma^{W^+W^-}_{W,H}$ and $\delta\Gamma^{W^+G^-}_W$ are the counterterms needed to remove the UV divergences contained in $\Gamma^{\mathrm{vertex}}_{W,H}$, $\Gamma^{W^+W^-}_{W,H}$ and $\Gamma^{W^+G^-}_W$. In what follows, we write the above one loop corrections explicitly. The expressions for the counterterms can be found in Sect. 4.

3.1 Vertex with u–u–d exchange: Fig. 2a$_1$

The amplitude of the u–u–d quarks contribution to $H^+A^0W^+$ vertex is given by

$$\Gamma^{uud}_H = N_\mathrm{C}\frac{\alpha}{2\pi\sqrt{2}M^2_{H^\pm}}Y_{uu} \times \Big((-m^2_d - 3M^2_{H^\pm} + m^2_u)Y^\mathrm{L}_{ud}B_0(M^2_{H^\pm}, m^2_d, m^2_u)$$

$$
\begin{aligned}
&+(m_d^2 - m_u^2) Y_{ud}^{\mathrm{L}} B_0(0, m_d^2, m_u^2) \\
&-2M_{H^\pm}^2 \{ (m_u^2 Y_{ud}^{\mathrm{L}} + m_d m_u Y_{ud}^{\mathrm{R}}) C_0 \\
&+Y_{ud}^{\mathrm{L}} [p_W^2 C_1 - 2C_{00} \\
&+(-M_A^2 + M_{H^\pm}^2 - p_W^2) C_{12} - 2M_A^2 C_{22}] \} \Big), \quad (3.5)
\end{aligned}
$$

$$
\begin{aligned}
\Gamma_W^{uud} &= N_{\mathrm{C}} \frac{\alpha}{\pi\sqrt{2}} \\
&\times Y_{uu} \Big(Y_{ud}^{\mathrm{L}} B_0(M_{H^\pm}^2, m_d^2, m_u^2) \\
&+m_u (m_u Y_{ud}^{\mathrm{L}} + m_d Y_{ud}^{\mathrm{R}}) C_0 \\
&-Y_{ud}^{\mathrm{L}} \{ (M_A^2 - M_{H^\pm}^2) C_1 + M_A^2 C_2 + 2C_{00} \\
&+(M_A^2 - M_{H^\pm}^2 + p_W^2) C_{11} \\
&+(3M_A^2 - M_{H^\pm}^2 + p_W^2) C_{12} + 2M_A^2 C_{22} \} \Big), \quad (3.6)
\end{aligned}
$$

with A_0, B_0, C_i and C_{ij} the Passarino–Veltman functions [21] which we define in Appendix A. $N_{\mathrm{C}} = 3$ for quarks and 1 for leptons. All the C_i and C_{ij} have the same arguments: $(p_W^2, M_{H^\pm}^2, M_A^2, m_u^2, m_d^2, m_u^2)$

3.2 Vertex with d–d–u exchange: Fig. 2a$_2$

The amplitude of this diagram can be obtained from the above one just by making the following replacement:

$$\Gamma_{H,W}^{ddu} = \Gamma_{H,W}^{uud} [m_u \longleftrightarrow m_d, \quad Y_{ud}^{\mathrm{R}} \longleftrightarrow Y_{ud}^{\mathrm{L}}, \quad Y_{uu} \to Y_{dd}].$$

The total contribution of the vertex is

$$\Gamma_{W,H}^{\mathrm{vertex}} = \Gamma_{W,H}^{uud} + \Gamma_{W,H}^{ddu}.$$

3.3 W^+–W^- self-energy: Fig. 2a$_3$

The contribution of the W self-energy Fig. 2a$_3$ evaluates to

$$
\begin{aligned}
\Gamma_H^{WW} &= \frac{N_{\mathrm{C}} \alpha}{2\pi s_{\mathrm{W}}^2 (p_W^2 - M_W^2)} \\
&\times \{ A_0(m_u^2) + m_d^2 B_0(p_W^2, m_d^2, m_u^2) \\
&-2B_{22}(p_W^2, m_d^2, m_u^2) \\
&+p_W^2 B_1(p_W^2, m_d^2, m_u^2) \}, \\
\Gamma_W^{WW} &= -\frac{N_{\mathrm{C}} \alpha}{4\pi s_{\mathrm{W}}^2 (p_W^2 - M_W^2)} \\
&\times \{ A_0[m_u^2] + m_d^2 B_0(p_W^2, m_d^2, m_u^2) \\
&-2B_{22}(p_W^2, m_d^2, m_u^2) \\
&+p_W^2 B_1(p_W^2, m_d^2, m_u^2) \\
&+2(M_{H^\pm}^2 - M_A^2)(B_1(p_W^2, m_d^2, m_u^2) \\
&+B_{21}(p_W^2, m_d^2, m_u^2) \}. \quad (3.7)
\end{aligned}
$$

3.4 W–G mixing: Fig. 2a$_4$

In accordance with Lorentz invariance, the mixing self-energy W–G is proportional to p_W^μ and evaluates to

$$
\begin{aligned}
\Gamma_W^{WG} &= \frac{N_{\mathrm{C}} \alpha (M_{H^\pm}^2 - M_A^2)}{4\pi M_W^2 s_{\mathrm{W}}^2 (p_W^2 - M_W^2)} \{ m_d^2 B_0(p_W^2, m_d^2, m_u^2) \\
&+[m_d^2 - m_u^2] B_1(p_W^2, m_d^2, m_u^2) \}, \\
\Gamma_H^{WG} &= 0. \quad (3.8)
\end{aligned}
$$

4 On-mass-shell renormalization

The parameters entering the tree-level amplitude in (2.4) are all standard model parameters (e and s_{W}). This fact will render the one loop renormalization rather simple, in the sense that all non-standard parameters appearing first at the one loop level (like $\tan\beta$), will not get renormalized. This is in contrast to the calculation in [22] for the process $H^+ \to hW^+$ which explicitly contains the factor $\cos^2(\beta - \alpha)$ at tree level. Therefore, renormalization conditions related to the definition of $\tan\beta$ are not explicitly needed here. We will need, however, to renormalize the electric charge, the Weinberg angle, the charged Higgs wave function, the CP odd Higgs wave function and the W gauge boson wave function. In our case the $W^\pm$ gauge boson mixes with the Goldstone boson $G^\pm$, by virtue of Lorentz invariance of the self-energy; therefore, $\Sigma_\mu^{G^+W^-}$ is proportional to p_μ^W and so if the W is on shell, the mixing would have a vanishing contribution, but in the off-shell case we have to take this mixing into account.

In what follows we will mainly follow the on-shell renormalization developed by Santos et al. [22] which is the generalization to the 2HDM of the Aoki et al. on-shell renormalization scheme [23,24]. The crucial point in this scheme is that all fields and masses are renormalized after the diagonalization of the bare mass matrices. Another important point in this scheme is that the gauge fixing is written in terms of the renormalized parameters and fields and as a consequence it does not contain any counterterm.

4.1 Vertex $H^+A^0W^+$ counterterm

To obtain the renormalized vertex $W^-A^0H^+$ vertex we have to make the following substitutions in (2.1):

$$
\begin{aligned}
&W_\mu \to Z_W^{1/2} W_\mu, && (4.1) \\
&H^\pm \to Z_{H^+H^+}^{1/2} H^\pm, && (4.2) \\
&A^0 \to Z_A^{1/2} A^0, \\
&e \to Z_e e = (1 + \delta Z_e) e, \\
&M_W^2 \to M_W^2 + \delta M_W^2, && (4.3) \\
&M_Z^2 \to M_Z^2 + \delta M_Z^2.
\end{aligned}
$$

Note that in the on-shell scheme, the Weinberg angle is defined as $s_{\mathrm{W}}^2 = 1 - M_W^2/M_Z^2$. Therefore, the counterterm of s_{W} is completely fixed by the counterterm of the W and Z boson masses and is given by

$$\frac{\delta s_{\mathrm{W}}}{s_{\mathrm{W}}} = -\frac{1}{2} \frac{c_W^2}{s_{\mathrm{W}}^2} \left(\frac{\delta M_W^2}{M_W^2} - \frac{\delta M_Z^2}{M_Z^2} \right). \quad (4.4)$$

Setting $Z^{1/2} = 1 + (1/2)\delta Z$, one obtains the following counterterm:

$$\delta\mathcal{L} = \frac{e}{2s_{\mathrm{W}}} W_\mu^+ \left(H^- \overset{\leftrightarrow}{\partial}{}^\mu A^0 \right) \quad (4.5)$$

$$\times \left(\frac{1}{2}\delta Z_W + \frac{1}{2}\delta Z_{A^0} + \frac{1}{2}\delta Z_{H^\pm H^\pm} + \delta Z_e - \frac{\delta s_{\rm W}}{s_{\rm W}} \right).$$

– In the on-mass-shell scheme the counterterms can be fixed by the following renormalization conditions: First, the on-shell condition for the charged Higgs boson $H^\pm$, CP odd A^0 and the W and Z gauge bosons. We choose to identify the physical mass with the corresponding parameter in the renormalized lagrangian, and require the residue of the propagator to have its tree-level value, i.e.,

$$\delta M^2 = {\rm Re}\Sigma(M^2) \;\; \text{and} \;\; \delta Z = -\frac{\partial \Sigma(k^2)}{\partial k^2}|_{k^2=M^2} \quad (4.6)$$

where $\Sigma(k^2)$ is the bare self-energy of the $H^\pm$, A^0 or W.
– The electric charge e is defined as in the minimal standard model [24,25].
– Tadpoles are renormalized in such a way that the renormalized tadpoles vanish: $T_h + \delta t_h = 0$, $T_H + \delta t_H = 0$. These conditions guarantee that $v_{1,2}$ appearing in the renormalized lagrangian are located at the minimum of the one loop potential.

Using these renormalization conditions and as is shown in [24], the renormalization constant of the electric charge and counterterm of gauge boson mass are given by

$$\begin{aligned} \delta Z_e &= -\frac{1}{2}\delta Z_{\gamma\gamma} + \frac{1}{2}\frac{s_{\rm W}}{c_W}\delta Z_{Z\gamma} \\ &= \frac{1}{2}\frac{\partial \Sigma_{\rm T}^{\gamma\gamma}(k^2)}{\partial k^2}|_{k^2=0} + \frac{s_{\rm W}}{c_W}\frac{\Sigma_{\rm T}^{\gamma Z}(0)}{M_Z^2}, \end{aligned} \quad (4.7)$$

$$\delta M_W^2 = \Sigma_{\rm T}^{WW}(M_W^2) \quad \text{and} \; \delta M_Z^2 = \Sigma_{\rm T}^{ZZ}(M_Z^2), \quad (4.8)$$

where $\Sigma_{\rm T}^{WW}$, $\Sigma_{\rm T}^{ZZ}$ $\Sigma_{\rm T}^{\gamma\gamma}$ are, respectively, the W, Z and photon self-energies depicted in Fig. 2b$_{4,5,6}$; the T index is to denote that we take only the transverse part. We stress at this stage that the fermionic contribution to the mixing $\Sigma_{\rm T}^{\gamma Z}(k^2)$ vanishes at $k^2 = 0$.

4.2 Counterterm for the W self-energy and the mixing W–G

One obtains the counterterm for the W–W self-energy by substituting (4.1) and (4.4) in the W lagrangian:

$$\begin{aligned} \delta(W^\mu W^\nu) = {\rm i}(g^{\mu\nu} - \frac{p_W^\mu p_W^\nu}{p_W^2})(\delta M_W^2 + (M_W^2 - p_W^2)\delta Z_W) \\ + {\rm i}\frac{p_W^\mu p_W^\nu}{p_W^2}(\delta M_W^2 + M_W^2 \delta Z_W). \end{aligned} \quad (4.9)$$

All the counterterms appearing in $\delta(W_\mu W_\nu)$ are fixed by the renormalization conditions fixed above (4.6) and (4.8). As we have mentioned above, the W^+ boson and the G^+ Goldstone mix. To treat this mixing, Santos et al. [22] have considered the mixing of G^+–H^-, which they have renormalized in the following way:

$$H^\pm \to Z_{H^+H^+}^{1/2} H^\pm + Z_{H^+G^+}^{1/2} G^\pm, \quad (4.10)$$

$$G^\pm \to Z_{G^+G^+}^{1/2} G^\pm + Z_{G^+H^+}^{1/2} H^\pm. \quad (4.11)$$

At the one loop level $Z_{ii}^{1/2} = 1 + 1/2\delta Z_{ii}$ and $Z_{ij}^{1/2} = \delta Z_{ij}$ where $\delta Z_{ij} = \mathcal{O}(\alpha)$. These four renormalization constants together with the counterterm mass of the charged Higgs bosons are fixed by imposing the on-shell condition (mass located at the pole of the propagator and residue equal to one) and the vanishing mixing both for the $\Sigma_{G^+H^+}(k^2)$ self-energy at $k^2 = M_{H^\pm}^2$ and the $\Sigma_{H^+G^+}(k^2)$ self-energy at $k^2 = 0$. Note that the Goldstone boson receives its renormalized mass from the gauge fixing lagrangian. Before introducing this lagrangian the Goldstone boson is massless, and so the renormalization conditions imposed on the propagator of the Goldstone and its mixing with charged Higgs boson will be fixed at $k^2 = 0$.

At the one loop level the renormalization constants $\delta Z_{H^+H^+}$ and $\delta Z_{G^+G^+}$ are given by

$$\begin{aligned} \delta Z_{H^+H^+} &= -\frac{\partial \Sigma_{H^+H^+}(k^2)}{\partial k^2}|_{k^2=M_{H^\pm}^2} \quad \text{and} \\ \delta Z_{G^+G^+} &= -\frac{\partial \Sigma_{G^+G^+}(k^2)}{\partial k^2}|_{k^2=0}. \end{aligned} \quad (4.12)$$

Performing the replacement (4.1), (4.4) and (4.11) in the W gauge fixing term ${\rm i}M_W \partial^\mu W_\mu^+ G^-$, generated from the covariant derivative, one finds the following counterterm for the mixing W^+–G^-:

$$\delta(W_\mu^+ G^-) = \frac{{\rm i}p_W^\mu M_W}{2}\left(\frac{\delta M_W^2}{M_W^2} + \delta Z_W + \delta Z_{G^+G^+}\right). \quad (4.13)$$

This completes the set of counterterms needed for our study. The renormalization constants of the wave function and the mass counterterms are given in Appendix B.

4.3 Back to counterterms form factors

After the short discussion in Sect. 4.2 about the on-shell renormalization we are using, we are now able to give the expressions of the counterterms $\delta\Gamma_{W,H}^{\rm vertex}, \delta\Gamma_{W,H}^{W^+W^-}$, $\delta\Gamma_W^{W^+G^-}$ defined in (3.3) and (3.4):

$$\begin{aligned} \delta\Gamma_W^{\rm vertex} &= -\left(\delta Z_e - \frac{\delta s_{\rm W}}{s_{\rm W}} + \frac{1}{2}(\delta Z_{H^+H^+} + \delta Z_{A^0} + \delta Z_W)\right), \\ \delta\Gamma_H^{\rm vertex} &= -2\delta\Gamma_W^{\rm vertex}, \\ \delta\Gamma_W^{WW} &= \{(M_{H^\pm}^2 + p_W^2 - m_A^2)\delta Z_W - \delta M_W^2 \\ &\quad - M_W^2 \delta Z_W\}/(p_W^2 - M_W^2), \\ \delta\Gamma_H^{WW} &= 2\{\delta M_W^2 + (M_W^2 - p_W^2)\delta Z_W\}/(p_W^2 - M_W^2), \\ \delta\Gamma_W^{WG} &= \frac{1}{2}(M_{H^\pm}^2 - M_A^2) \\ &\quad \times \left\{ \frac{\delta M_W^2}{M_W^2} + \delta Z_W + \delta Z_{G^+G^+} \right\}/(p_W^2 - M_W^2). \end{aligned} \quad (4.14)$$

5 Numerical results and discussion

In the previous section we have summarized the analytical formulae for the fermionic $\mathcal{O}(\alpha)$ radiative correction to

the decay $H^+ \to W^+ A^0$. In this section we focus on the numerical analysis. We take the following experimental input for the physical parameters [26]:

- the fine structure constant: $\alpha = e^2/4\pi = 1/137.03598$.
- the gauge boson masses: $M_Z = 91.187\,\mathrm{GeV}$, $M_W = 80.41\,\mathrm{GeV}$ and $\Gamma_W = 2.06\,\mathrm{GeV}$,
- the input lepton masses: $m_e = 0.511\mathrm{MeV}$, $m_\mu = 0.1057\,\mathrm{GeV}$, $m_\tau = 1.784\,\mathrm{GeV}$
- for the light quark masses we use the effective values which are chosen in such a way that the experimentally extracted hadronic part of the vacuum polarizations is reproduced [27]:

$$m_d = 47\,\mathrm{MeV} \quad m_u = 47\,\mathrm{MeV} \quad m_s = 150\,\mathrm{MeV},$$
$$m_c = 1.55\,\mathrm{GeV} \quad m_b = 4.5\,\mathrm{GeV}.$$

For the top quark mass we take $m_t = 175\,\mathrm{GeV}$. In the on-shell scheme we consider, $\sin^2\theta_\mathrm{W}$ is given by $\sin^2\theta_\mathrm{W} \equiv 1 - M_W^2/M_Z^2$, and this expression is valid beyond tree level.

In the on-shell case it can be shown that the interference term $2\mathrm{Re}\mathcal{M}^{0*}\mathcal{M}^1$, found from squaring the one loop corrected amplitude $|\mathcal{M}^0 + \mathcal{M}^1|^2$, is equal to $\Gamma_H|\mathcal{M}^0|^2$. Hence the one loop corrected width Γ^1_on can be written as

$$\Gamma^1_\mathrm{on} = (1 + \Gamma_H)\Gamma^0_\mathrm{on},$$

with Γ_H (defined by (3.4) being interpreted as the fractional contribution to the tree-level width, Γ^0_on. Note that Γ_W (3.3) does not contribute to Γ^1_on. In the off-shell case, and taking the final state fermions to be massless, $2Re\mathcal{M}^{0*}\mathcal{M}^1$ is again equal to $\Gamma_H|\mathcal{M}^0|^2$, although Γ_H now has a dependence on E_1 and E_2 and thus cannot be factorized out of the phase space integral. Therefore, we define the fractional contribution to the tree-level width as $\delta\Gamma_\mathrm{off}$, with

$$\Gamma^1_\mathrm{off} = (1 + \delta\Gamma_\mathrm{off})\Gamma^0_\mathrm{off}.$$

Since Γ_W does not contribute to the corrected matrix element it is evident that the W^+G^+ mixing has a vanishing contribution and is given in Sect. 3.3 for completeness.

We now briefly consider the constraints on the masses of the Higgs bosons that can be extracted from current precision measurements of the ρ parameter. In the SM (and 2HDM) ρ is defined by $\rho = M_W^2/(M_Z^2\cos^2\theta_\mathrm{W}) = 1$ to all orders. This definition of the ρ parameter can regarded as the on-shell definition of the Weinberg angle to all orders. When new physics (say coming from the 2HDM) is present, and in order to keep the correct on-shell definition of ρ parameter, the static 2HDM contributions [28] are constrained by $-0.0017 \leq \delta\rho \leq 0.0027$ at the 2σ level [29].

Imposing this condition and using the formulae in [28] we plot in Fig. 3 the allowable values of $M_{H^\pm}$ and M_A. We vary all Higgs masses up to 500 GeV and respect the current experimental lower limits for 5000 randomly chosen values. In Fig. 3 the triangles (points) disallow (allow) the decay $H^\pm \to AW^*$. From the figure we can clearly see that for $M_{H^\pm} \geq 100\,\mathrm{GeV}$ the vast majority of the allowed parameter space satisfies $M_{H^\pm} \geq M_A$, thus implying that the decay $H^\pm \to AW^{(*)}$ will be open for $M_{H^\pm}$ which is of interest at the LHC and the Tevatron. For $M_{H^\pm} \leq 100\,\mathrm{GeV}$ (i.e. the LEP-II range) it is easier to find $M_{H^\pm} \leq M_A$.

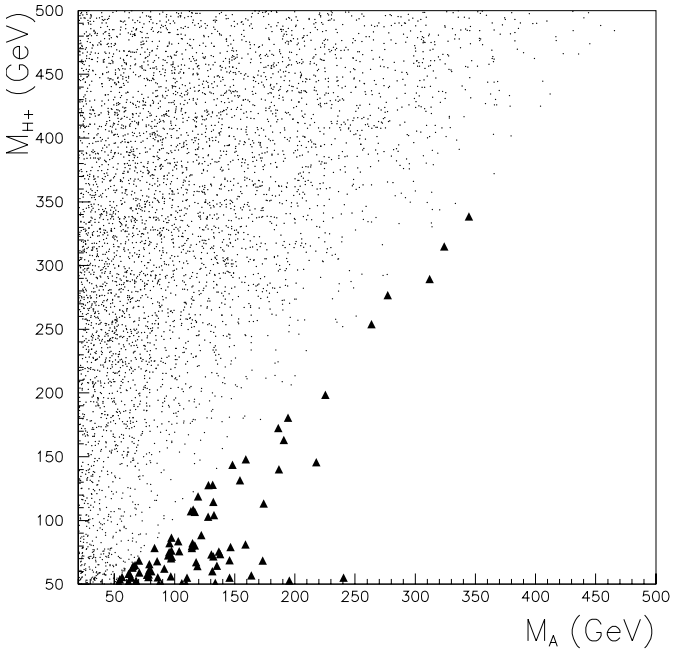

Fig. 3. Scatter plot of values of $M_{H^\pm}$ and M_A consistent with measurements of ρ. Triangles disallow the decay $H^\pm \to AW^{(*)}$

5.1 On-shell W gauge boson

We now present our results for the case of the W boson being on shell. There are three unknown parameters which determine the magnitude of the one loop corrected width Γ^1_on: $M_{H^\pm}$, M_A and $\tan\beta$. This is in contrast to the decay $H^\pm \to hW$ in which the mixing angle α and the mass of the heavier CP even Higgs boson (H) enter the calculation [22]. We stress that this latter analysis only considered the top–bottom loops, while we include all the fermion corrections and find that the light fermion loops are not entirely negligible. Moreover, there can be significant interference among the various contributions, both destructive and constructive. We consider both Model I and Model II, which have effectively identical results at small $\tan\beta$, although they differ at large $\tan\beta$.

Let us discuss first the effect of a relatively light charged Higgs ($M_{H^\pm} < 250\,\mathrm{GeV}$) and a very light CP odd ($M_A \approx 35\,\mathrm{GeV}$) on Γ_H. In Fig. 4 we plot Γ_H (fractional correction to the tree-level width) in Model II as a function of $M_{H^\pm}$ for several values of $\tan\beta$. We note first that for a fixed value of $\tan\beta$, Γ_H is insensitive to the variation in M_A when $M_{H^\pm}$ is varied from 120 to 260 GeV. The peaks correspond to the opening of the decay $H^+ \to \bar{t}b$. For small $\tan\beta$ and $M_{H^\pm} < 170\,\mathrm{GeV}$ the correction is rather small ($\approx 2\%$); when $M_{H^\pm} > 180\,\mathrm{GeV}$ one can reach a correction of 10%. In the case where $\tan\beta$ is large, the effect comes exclusively from the bottom quark mass and is around 10%.

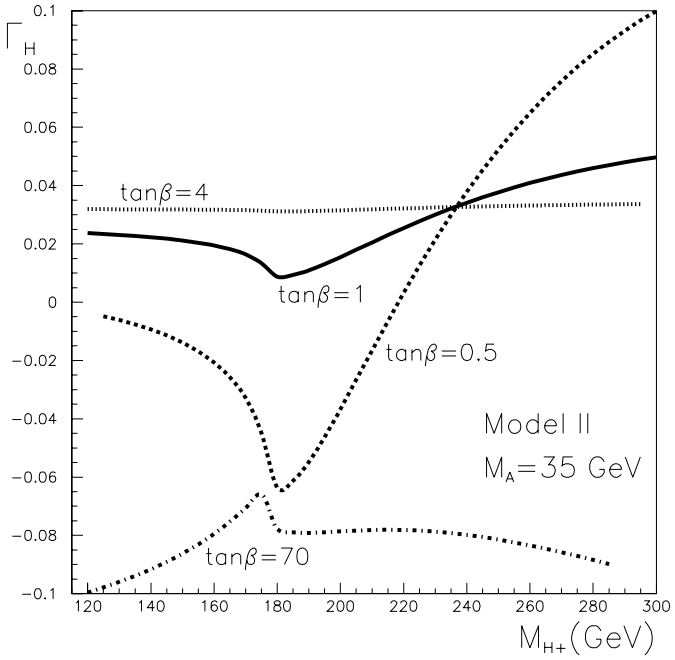

Fig. 4. Γ_H as a function of $M_{H^\pm}$ (Model II) for $M_A = 35\,\mathrm{GeV}$, $\tan\beta = 0.5$, 1.0, 4 and 70

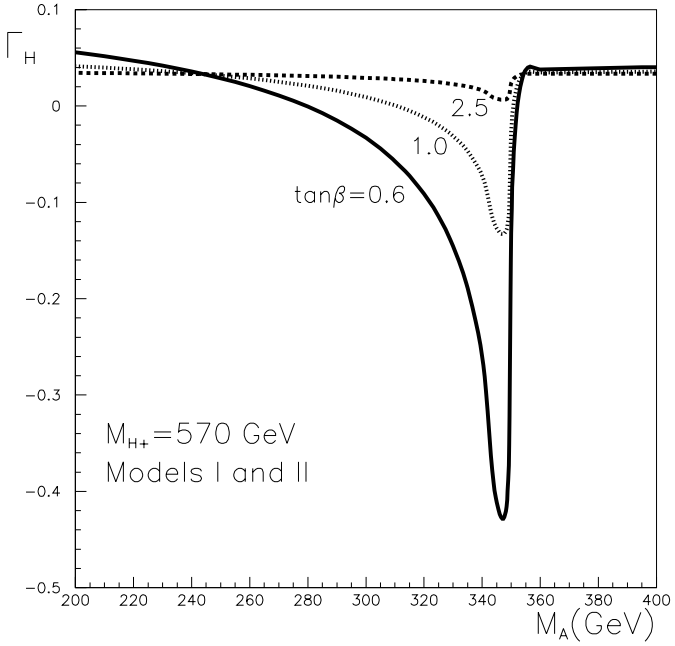

Fig. 5. Γ_H as a function of M_A (Models I and II) for $\tan\beta = 0.6$, 1.0 and 2.5

In Fig. 5 we plot Γ_H as a function of M_A, taking $M_{H^\pm} = 570\,\mathrm{GeV}$ and three small values of $\tan\beta$. Since we are not considering a large $\tan\beta$ this plot is relevant for both Model I and II. For M_A less than 300 GeV or heavier than 360 GeV the effect is about 5%. When M_A becomes close to $2m_t$ a sharp peak appears, and this corresponds to the opening of the channel $A^0 \to t\bar{t}$, the maximal effect in this case being around 50%. For M_A away from this threshold value ($M_A \approx 330 \to 345\,\mathrm{GeV}$) and for small

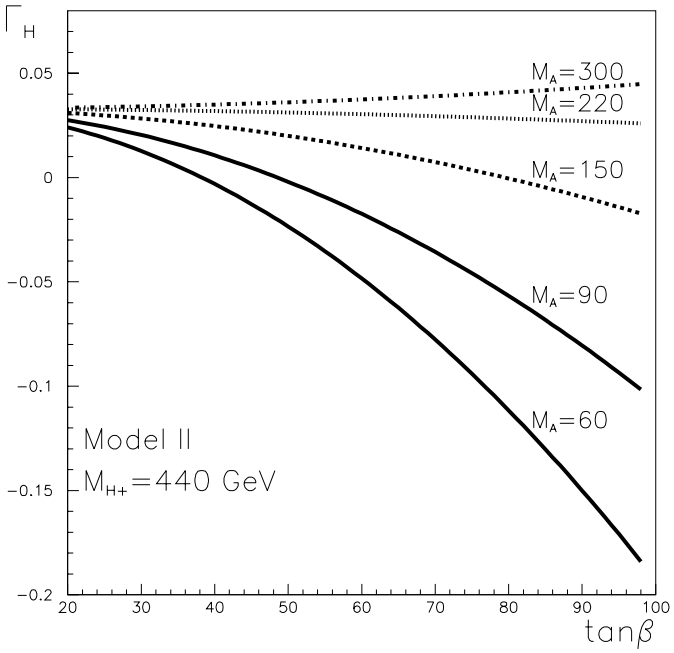

Fig. 6. Γ_H as a function of $\tan\beta$ (Model II) for $\tan\beta \geq 20$

$\tan\beta$ one can have a correction of about $-14\% \to -41\%$. As $\tan\beta$ increases one quickly approaches a horizontal line at 3.3%. These effects are explained as follows: the *ttb* loop correction is proportional to Y_{uu} and dominates the *bbt* loop correction at small $\tan\beta$ because $m_t \gg m_b$. Since Y_{uu} is proportional to $1/\tan\beta$ we can explain the $\tan\beta$ dependence in Fig. 5. As $\tan\beta$ increases the contribution of the *ttb* loop weakens rapidly and the dominant contribution to the corrected width becomes that of the renormalized e and s_W, giving a fixed value of $\Gamma_H \approx 3.3\%$ which is very insensitive to $\tan\beta$ (note that the *bbt* loop in Model II is proportional to $\tan\beta$ – see below). We do not notice an obvious correlation between $M_{H^\pm}$ and Γ_H; for the optimal case considered of $\tan\beta = 0.5$ and $M_A \approx 330\,\mathrm{GeV}$, varying $M_{H^\pm}$ from 450 GeV to 800 GeV causes Γ_H to fall from -18% to -27%.

In Fig. 6 we plot Γ_H in Model II as a function of $\tan\beta$ for $\tan\beta \geq 20$. In Model I all the fermion loops decouple as $\tan\beta$ increases and one has $\Gamma_H \approx 3.3\%$ for $\tan\beta \geq 4$. In Model II the *bbt* loop dominates with increasing $\tan\beta$ and for $\tan\beta \geq 20$ the value of Γ_H starts to differ from the corresponding value in Model I. Again one can find sizable negative corrections, with the largest occurring for smaller M_A, i.e. the closer M_A is to $2m_b$, the more on shell the virtual b quarks are.

In Fig. 7 we show graphically the relative magnitude of the sum of the heavy quark loops, *ttb* and *bbt*, compared to the sum of the remaining fermion loops (Γ_light). Since we plot only low values of $\tan\beta$ the *ttb* contribution dominates the *bbt* loop and so we label the sum of the *ttb* and *bbt* contributions as Γ_{ttb}. One can see that Γ_light is of comparable strength to the heavy quark loops unless M_A is close to $2m_t$. In addition there can be constructive or destructive interference, which is shown in Fig. 7 by the sign of the ratio.

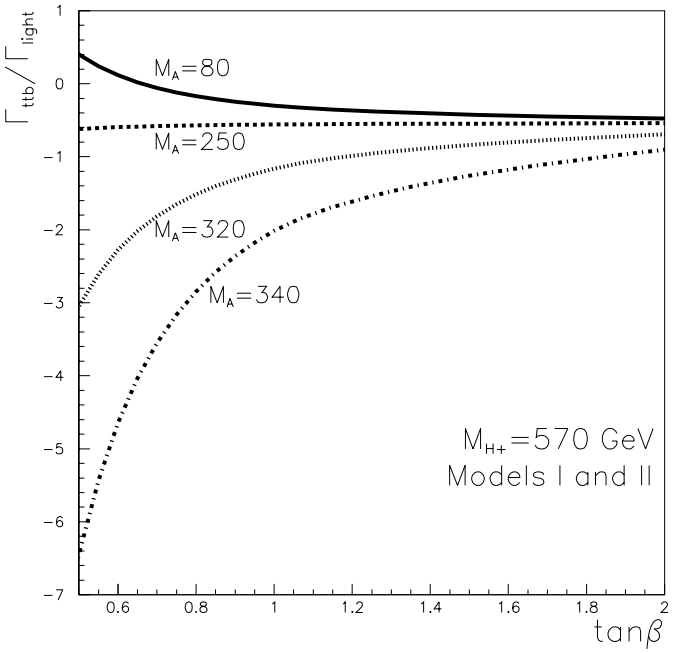

Fig. 7. $\Gamma_{ttb}/\Gamma_{\rm light}$ as a function of small $\tan\beta$ for several values of M_A (Models I and II)

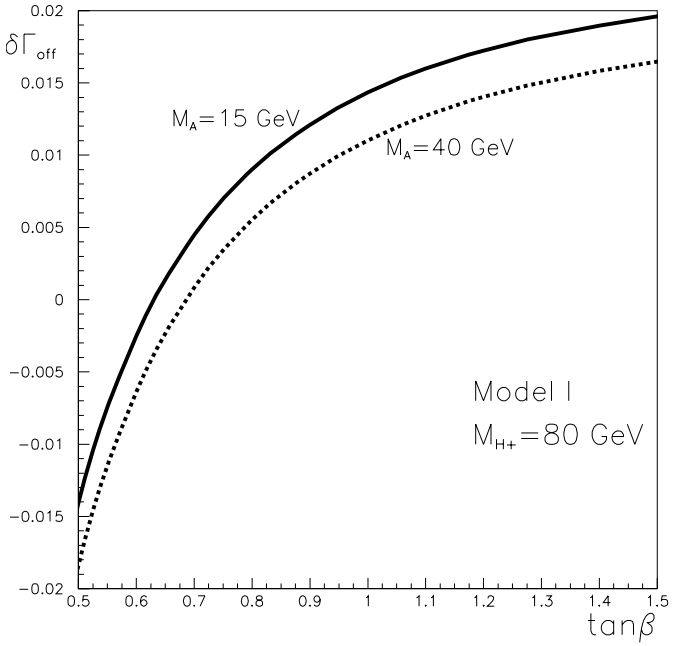

Fig. 8. $\delta\Gamma_{\rm off}$ as a function of small $\tan\beta$ and for $M_A = 15$, 40 GeV (Model I)

5.2 Off-shell W gauge boson

We now consider the case of the W gauge boson being off shell. Since the decay $H^\pm \to AW^*$ is possible for a light $H^\pm$ in range at LEP-II we shall present results for $M_{H^\pm} = 80\,\text{GeV}$, which is also in the mass region considered problematic for detection channels which make use of the conventional decays $H^\pm \to \tau\nu_\tau$, cs. As is mentioned in the introduction, charged Higgs bosons of Model II are excluded from the LEP-II discovery range by precision measurements of $b \to s\gamma$. Our discussion will therefore be focussed on Model I. In the massless fermion final state limit, the WW self-energy is the only additional contribution to the one loop corrected width for the off-shell decay[1]. The WW self-energy is the standard diagram and does not depend on $\tan\beta$. Hence all the $\tan\beta$ dependence is contained in the vertex contribution and in the case of Model I it is enhanced when $\tan\beta$ is small.

In Fig. 8 we plot the magnitude of the one loop corrections, $\delta\Gamma_{\rm off}$, as a function of small $\tan\beta$ for two values of M_A. We can see that for $\tan\beta \geq 2$ one approaches a fixed value ($\approx 2\%$) for $\delta\Gamma_{\rm off}$ – this is to be interpreted (as before) as the fermion loops decoupling, leaving a $\tan\beta$ independent value which comes from the WW self-energy and from the renormalized e and $s_{\rm W}$ in the vertex contribution counterterms. For low $\tan\beta$ the one loop corrections are pulled negative. Very large corrections of up to -90% are possible for exceptionally small (≈ 0.1) values of $\tan\beta$, although such values are strongly disfavored by measurements of R_b which require $\tan\beta \geq 1.8$ (95% c.l.) for $M_{H^\pm} = 85\,\text{GeV}$ [8].

[1] Note that for the W being off shell, there are extra contributions coming from box diagrams which will be considered in [30]

6 Conclusions

We have computed the Yukawa coupling corrections to the decay $H^+ \to A^0 W^+$ in the case of an on-shell and off-shell W gauge boson. We have included in our analysis both top–bottom contributions and light fermion contributions, the latter being non-negligible. These may interfere destructively or constructively with the former. Restrictions on the possible values of the Higgs boson masses from considering the ρ parameter were also included and were found to give in the majority of the cases $M_{H^\pm} > M_A$. In the on-shell case, we studied the sensitivity of the Yukawa corrections to $\tan\beta$, and found similar effects for small $\tan\beta$ in both Model I and Model II, which can reach 50% for $m_A \approx 2m_t$. For large $\tan\beta$, in Model I all the fermion corrections decouple and reach a constant value of 3.3% for $\tan\beta > 4$; in Model II, the top mass effect is suppressed while the bottom mass effect is increased for $\tan\beta > 20$, allowing sizeable corrections of 10% or greater. For the case of the W gauge boson being off shell, the charged Higgs bosons in the LEP-II range and $\tan\beta$ not too small, the corrections are rather small and do not surpass 2%.

Acknowledgements. We thank A. Djouadi for his critical reading of the present manuscript. A. Akeroyd was supported by DGICYT under grants PB95-1077, by the TMR network grant ERBFMRXCT960090 of the European Union, and by a CSIC-UK Royal Society fellowship. A. Arhrib is very grateful to the Laboratoire de Physique Mathématique et Théorique de Mont-

pellier for its kind hospitality during his visit where part of this work has been done.

Appendix A: Passarino–Veltman functions

Let us recall the definitions of the scalar and tensor integrals [21] we use.

A.1 One point function

The one point function is defined by

$$A_0(m_0^2) = \frac{(2\pi\mu)^{4-d}}{\mathrm{i}\pi^2}\int \mathrm{d}^d q \frac{1}{[q^2 - m_0^2]};$$

μ is an arbitrary renormalization scale.

$$A_0(m_0^2) = m_0^2\,[1 + \Delta_0] + \mathcal{O}(d-4). \tag{A.1}$$

The UV divergences are contained in Δ_0 which is given by

$$\Delta_i = \frac{2}{4-d} - \gamma_E + \log(4\pi) + \log\frac{\mu^2}{m_i^2}; \tag{A.2}$$

note that in dimensional regularization $A_0(0) = 0$.

A.2 Two point functions

The two points functions are defined by

$$B_{0,\mu,\mu\nu}(p_1^2, m_0^2, m_1^2) = \frac{(2\pi\mu)^{4-d}}{\mathrm{i}\pi^2} \times \int \mathrm{d}^d q \frac{1, q_\mu, q_{\mu\nu}}{[q^2 - m_0^2][(q+p_1)^2 - m_1^2]}.$$

We have

$$B_0 = \frac{1}{2}(\Delta_0 + \Delta_1) - \int_0^1 \mathrm{d}x \mathrm{Log}\frac{x^2 p_1^2 - x(p_1^2 - m_0^2 + m_1^2) + m_1^2 - \mathrm{i}\epsilon}{m_0 m_1}. \tag{A.3}$$

The derivative of the B_0 function is defined as

$$B_0^{'}[X, m_1^2, m_2^2] = \frac{\partial}{\partial p^2} B_0[p^2, m_1^2, m_2^2]|_{p^2=X}.$$

Note that A_0 can be expressed in terms of B_0:

$$A_0(m^2) = m^2 + m^2 B_0(0, m^2, m^2).$$

Using Lorentz invariance, we have

$$B_\mu = p_{1\mu} B_1,$$
$$B_{\mu\nu} = p_{1\mu} p_{1\nu} B_{21} + g_{\mu\nu} B_{22}.$$

A.3 Three point functions

The three point functions are defined as

$$C_{0,\mu,\mu\nu}(p_1^2, p_{12}^2, p_2^2, m_0^2, m_1^2, m_2^2) = \frac{1}{\mathrm{i}\pi^2}\int \mathrm{d}^n q \frac{1, q_\mu, q_\mu q_\nu}{[q^2 - m_0^2][(q+p_1)^2 - m_1^2][(q+p_2)^2 - m_2^2]},$$

where $p_{12}^2 = (p_1 + p_2)^2$. Using Lorentz invariance, C_μ and $C_{\mu\nu}$ can be written as

$$C_\mu = p_{1\mu} C_1 + p_{2\mu} C_2, \tag{A.4}$$
$$C_{\mu\nu} = g_{\mu\nu} C_{00} + p_{1\mu} p_{1\nu} C_{11} + p_{2\mu} p_{2\nu} C_{22} + (p_{1\mu} p_{2\nu} + p_{2\mu} p_{1\nu}) C_{12}. \tag{A.5}$$

Appendix B: Renormalization constants

Here we give all the renormalization constants necessary to compute the counterterms defined in (4.15).

B.1 Gauge bosons self-energies

Let $\mathrm{i}e\gamma^\mu(V_L(1-\gamma_5)/2 + V_R(1+\gamma_5)/2)$ be the general coupling of the gauge bosons V_μ to a pair of fermions f and f'. The coefficient of $-g_{\mu\nu}$ of the self-energy of the gauge boson V_μ is given by

$$\begin{aligned}\Sigma_{\mathrm{T}}^{VV}(p^2) = -\frac{N_{\mathrm{C}}\alpha}{2\pi}\{&({V_L}^2 + {V_R}^2)[A_0(m_{f'}^2) \\ &-2B_{22}(p^2, m_{f'}^2, m_f^2) + p^2 B_1(p^2, m_{f'}^2, m_f^2)] \\ &+m_f[m_f({V_L}^2 + {V_R}^2) - 2m_{f'} V_L V_R] \\ &\times B_0(p^2, m_{f'}^2, m_f^2)\}.\end{aligned} \tag{B.1}$$

We have

- $V = Z$, $f = f'$, $Z_L = -1/(s_{\mathrm{W}} c_W)(T_f - e_f s_{\mathrm{W}}^2)$, $Z_R = (e_f s_{\mathrm{W}}^2)/(s_{\mathrm{W}} c_W)$, with $T_u = 1/2$ and $T_d = -1/2$.
- $V = \gamma$, $f = f'$, $\gamma_L = \gamma_R = -e_f$.
- $V = W$, $f = u$ and $f' = d$ $W_L = -1/(2^{1/2} s_{\mathrm{W}})$, $W_R = 0$.

The renormalization constant of the electric charge is given by

$$\begin{aligned}\delta Z_e = -\frac{1}{2}\delta Z_{\gamma\gamma} &= \frac{1}{2}\frac{\partial \Sigma_{\mathrm{T}}^{\gamma\gamma}(k^2)}{\partial k^2}|_{k^2=0} \\ &= \frac{1}{2}\frac{N_{\mathrm{C}}\alpha}{3\pi}\left\{ e_d^2\left[-\frac{1}{3} + B_0(0, m_d^2, m_d^2) + 2m_d^2 B_0^{'}(0, m_d^2, m_d^2)\right],\right. \\ &\left. + e_u^2\left[-\frac{1}{3} + B_0(0, m_u^2, m_u^2) + 2m_u^2 B_0^{'}(0, m_u^2, m_u^2)\right]\right\}.\end{aligned} \tag{B.2}$$

The mass counterterms for the gauge boson W and Z are given by

$$\delta M_W^2 = \Sigma_{\mathrm{T}}^{WW}(p^2 = M_W^2),$$
$$\delta M_Z^2 = \Sigma_{\mathrm{T}}^{ZZ}(p^2 = M_Z^2). \tag{B.3}$$

B.2 Wave function renormalization

The wave function renormalization constants for the W gauge boson can be obtained from the self-energy as

$$\begin{aligned}\delta Z_W &= -\frac{\partial \Sigma_{\rm T}^{WW}(k^2)}{\partial k^2}|_{k^2=M_W^2} \\ &= \frac{\alpha}{4\pi M_W^2 s_{\rm W}^2}\{M_W^2/3 + (m_d^2 - m_u^2)^2 \\ &\quad \times B_0(0, m_d^2, m_u^2)/M_W^2 \\ &\quad -(m_d^2 - m_u^2)^2 + M_W^4)B_0(M_W^2, m_d^2, m_u^2)/M_W^2 \\ &\quad +[(m_d^2 - m_u^2)^2 + m_u^2 M_W^2 - 2M_W^4 + 2m_d^2 M_W^2]B_0' \\ &\quad \times (M_W^2, m_d^2, m_u^2)\}. \qquad \text{(B.4)}\end{aligned}$$

The renormalization constants of the charged Higgs, CP odd Higgs and the Goldstone boson wave function are given by

$$\begin{aligned}\delta Z_{H^+H^+} &= \frac{N_{\rm C}\alpha}{4\pi}(-({Y_{ud}^{\rm L}}^2 + {Y_{ud}^{\rm R}}^2)B_0(M_{H\pm}^2, m_d^2, m_u^2) \\ &\quad +([m_d^2 + m_u^2 - M_{H^\pm}^2]({Y_{ud}^{\rm L}}^2 + {Y_{ud}^{\rm R}}^2) \\ &\quad +4m_d m_u Y_{ud}^{\rm L} Y_{ud}^{\rm R})B_0'(M_{H^\pm}^2, m_d^2, m_u^2)), \\ \delta Z_{A^0} &= -N_{\rm C}\frac{\alpha}{2\pi}\{Y_{dd}^2[B_0(M_A^2, m_d^2, m_d^2) \\ &\quad +M_A^2 B_0^{'}(M_A^2, m_d^2, m_d^2)] \\ &\quad +Y_{uu}^2[B_0(M_A^2, m_u^2, m_u^2) \\ &\quad +M_A^2 B_0^{'}(M_A^2, m_u^2, m_u^2)]\}, \qquad \text{(B.5)} \\ \delta Z_{G^+G^+} &= \frac{\alpha N_{\rm C}}{8\pi M_W^2 s_{\rm W}^2}\{-(m_d^2 + m_u^2)B_0(0, m_d^2, m_u^2) \\ &\quad +(m_d^2 - m_u^2)^2 B_0^{'}(0, m_d^2, m_u^2)\}.\end{aligned}$$

References

1. P.W. Higgs, Phys. Lett. B **12**, 132 (1964); Phys. Rev. Lett. **13**, 508 (1964)
2. S. Weinberg, Phys. Rev. Lett. **19**, 1264 (1967); S. Glashow, Nucl. Phys. **20**, 579 (1961); A. Salam, in Elementary Particle Theory, edited by N. Svartholm (1968) p. 367
3. J.F. Gunion, H.E. Haber, G.L. Kane, S. Dawson, The Higgs hunter's guide (Addison-Wesley, Reading 1990)
4. A.G. Akeroyd, Nucl. Phys. B **544**, 557 (1999)
5. Delphi Collaboration, P. Abreu et al., Phys. Lett. B **420**, 140 (1998)
6. OPAL Collaboration, G. Abbiendi et al., Eur. Phys. J. C **7**, 407 (1999)
7. F. Abe et al., CDF Collaboration, Phys. Rev. Lett. **79**, 357 (1997)
8. M. Ciuchini, G. Degrassi, P. Gambino, G.F. Giudice, Nucl. Phys. B **527**, 21 (1998)
9. F.M. Borzumati, C. Greub, PM/98/23, (hep-ph/9810240); Phys. Rev. D **58**, 074004 (1998); Phys. Rev. D **59**, 057501 (1999)
10. D. Bowser-Chao, K. Cheung, Wai-Yee Keung, UCD-HEP-98-30 (hep-ph/9811235); D. Atwood, L. Reina, A. Soni, Phys. Rev. D **55**, 3156 (1997)
11. Y. Grossman, Nucl. Phys. B **426**, 355 (1994); F.M. Borzumati, A. Djouadi, PM-98-1 (hep-ph/9806301)
12. M. Drees, E.A. Ma, P.N. Pandita, D.P. Roy, S.K. Vempati, Phys. Lett. B **433**, 346 (1998)
13. M.A. Diaz, E. Torrente–Lujan, J. Valle, IFIC/98/55, (hep-ph/9808412) Nuclear Physics B (in press)
14. S. Glashow, S. Weinberg, Phys. Rev. D **15**, 1958 (1977)
15. A. Djouadi, J. Kalinowski, P. Zerwas, Z. Phys. C **70**, 435 (1996)
16. L3 Collaboration, M. Acciarri et al., Phys. Lett. B **436**, 389 (1998)
17. G. 't Hooft, M. Veltman, Nucl. Phys. B **44**, 189 (1972); P. Breitenlohner, D. Maison, Commun. Math. Phys. **52**, 11 (1977)
18. H. Eck, J. Kublbeck, Guide to FeynArts 1.0, University of Wurzburg, 1992
19. R. Mertig, Guide to FeynCalc 1.0, University of Wurzburg, 1992
20. G.J. van Oldenborgh, Comput. Phys. Commun. **66**, 1 (1991)
21. G. Passarino, M. Veltman, Nucl. Phys. B **160**, 151 (1979); G. 't Hooft, M. Veltman, Nucl. Phys. B **153**, 365 (1979)
22. R. Santos, A. Barroso, Phys. Rev. D **56**, 5366 (1997); R. Santos, A. Barroso, L. Brucher, Phys. Lett. B **391**, 429 (1997)
23. K.I. Aoki, Z. Hioki, R. Kawabe, M. Konuma, T. Muta, Prog. Theo. Phys. **64**, 707 (1980); **65**, 1001 (1981); Suppl. Prog. Theo. Phys. **73**, 1 (1982)
24. A. Denner, Fortsch. Phys. **41**, 307 (1993)
25. M.Böhm, W. Hollik, H. Spiesberger, Fortschr. Phys. **34**, 11 (1986)
26. C. Caso et al., Eur. Phys. J. C **3**, 1 (1998)
27. S. Eidelman, F. Jegerlehner, Z. Phys. C **67**, 585 (1995); H. Burkhardt, B. Pietrzyk, Phys. Lett. B **356**, 398 (1995)
28. A. Denner, R.J. Guth, W. Hollik, J.H. Kuhn, Z. Phys. C **51**, 695 (1991)
29. J. Erler, P. Langacker, talk given at the 5th International Wein Symposium (WEIN 98), Santa Fe, June 1998 (hep-ph/9809352)
30. A. Akeroyd, A. Arhrib, E. Naimi, in preparation